

Zeitschrift: IABSE reports of the working commissions = Rapports des commissions de travail AIPC = IVBH Berichte der Arbeitskommissionen

Band: 29 (1979)

Artikel: Plastic analysis of reinforced concrete panels in frames

Autor: Sims, P.A.C.

DOI: <https://doi.org/10.5169/seals-23539>

Nutzungsbedingungen

Die ETH-Bibliothek ist die Anbieterin der digitalisierten Zeitschriften auf E-Periodica. Sie besitzt keine Urheberrechte an den Zeitschriften und ist nicht verantwortlich für deren Inhalte. Die Rechte liegen in der Regel bei den Herausgebern beziehungsweise den externen Rechteinhabern. Das Veröffentlichen von Bildern in Print- und Online-Publikationen sowie auf Social Media-Kanälen oder Webseiten ist nur mit vorheriger Genehmigung der Rechteinhaber erlaubt. [Mehr erfahren](#)

Conditions d'utilisation

L'ETH Library est le fournisseur des revues numérisées. Elle ne détient aucun droit d'auteur sur les revues et n'est pas responsable de leur contenu. En règle générale, les droits sont détenus par les éditeurs ou les détenteurs de droits externes. La reproduction d'images dans des publications imprimées ou en ligne ainsi que sur des canaux de médias sociaux ou des sites web n'est autorisée qu'avec l'accord préalable des détenteurs des droits. [En savoir plus](#)

Terms of use

The ETH Library is the provider of the digitised journals. It does not own any copyrights to the journals and is not responsible for their content. The rights usually lie with the publishers or the external rights holders. Publishing images in print and online publications, as well as on social media channels or websites, is only permitted with the prior consent of the rights holders. [Find out more](#)

Download PDF: 21.02.2026

ETH-Bibliothek Zürich, E-Periodica, <https://www.e-periodica.ch>

Plastic Analysis of Reinforced Concrete Panels in Frames

Analyse plastique d'éléments d'un cadre, composés de panneaux en béton armé

Plastische Berechnung von durch Rahmen umschlossenen Wandelementen aus Stahlbeton

P.A.C. SIMS

Senior Scientific Officer
Building Research Establishment
Watford, England

SUMMARY

Plastic analysis of reinforced concrete panels in frames is considered by assuming that recently identified collapse modes for unreinforced panels are also applicable to reinforced panels.

Two of these modes, shear mode S and shear-rotation mode SR, are shown to be valid by obtaining upper and lower bound solutions. The direct compression mode DC is shown to be valid only for a very restrictive range of panels with considerable differences existing between the upper and lower bound solutions.

RESUME

L'analyse plastique des panneaux en béton armé, éléments d'un cadre, est faite en supposant que les modes de rupture récemment identifiés pour les panneaux en béton sans armature sont également applicables aux panneaux en béton armé. La validité de deux de ces modes — le mode de cisaillement S et le mode de cisaillement-rotation SR — est démontrée à l'aide des solutions cinématiques et statiques correspondantes. Le mode de compression-directe DC n'est valable que pour une série très limitée de panneaux, avec des différences considérables entre les valeurs inférieures et supérieures de la charge ultime.

ZUSAMMENFASSUNG

Von der Annahme ausgehend, dass die vor kurzem gefundenen Kollapszustände für unbewehrte Wandelemente auch für den Fall bewehrter Elemente anwendbar sind, werden Wandelemente aus Stahlbeton, die durch Rahmen umschlossen sind, mit Hilfe der Plastizitätstheorie untersucht. Die Gültigkeit von zweien dieser Zustände, kurz als Typ S (Schiebung) beziehungsweise SR (Schiebung-Rotation) bezeichnet, wird mit Hilfe kinematischer und statischer Lösungen nachgewiesen. Wie gezeigt wird, tritt der dritte betrachtete Zustand, Typ DC (direkte Abstützung), nur für eine sehr beschränkte Auswahl von Wandelementen auf. Hier bestehen erhebliche Unterschiede zwischen den erhaltenen oberen und unteren Grenzwerten für die Traglast.



1. INTRODUCTION

Where wall panels are built in-line with frameworks, the resistance to in-plane horizontal loads increases considerably due to composite action between the frame and the panel. From the few known full-scale tests to destruction and many more model tests on unreinforced panels at the Building Research Station [1], [2], distinct collapse modes could be identified and idealised, Fig 1.

A theory to distinguish between these modes and their associated collapse loads for unreinforced panels has only recently been published by Wood [3], based on plasticity theory, which predicted these modes in their correct order of increasing relative frame/panel strength.

The small number of tests relating to reinforced panels has meant that the different collapse modes have not necessarily been observed and thus this paper extends Wood's approach by assuming that the idealised unreinforced panel modes can be applied to reinforced panels.

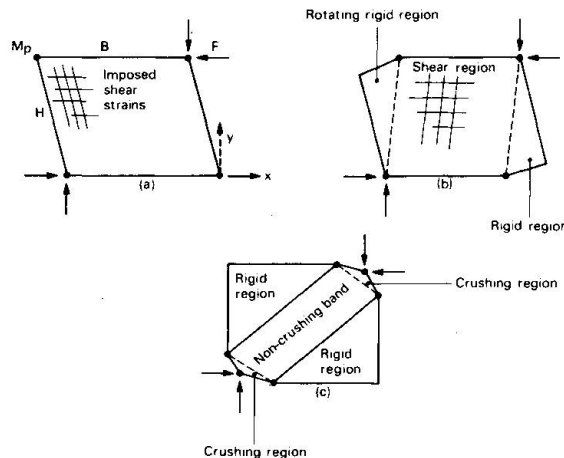


Fig 1 Idealised plastic failure modes
 (a) Shear mode S ; (b) Shear rotation mode SR ; (c) Corner crushing diagonal mode DC

2. PLASTICITY THEORY OF REINFORCED PANELS SUBJECT TO IN-PLANE HORIZONTAL LOADS

2.1 Yield criterion

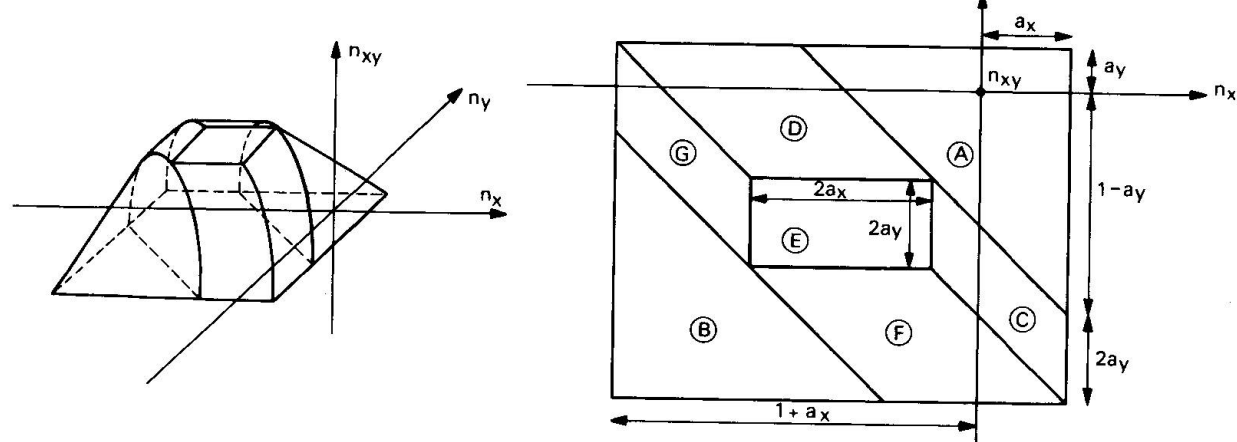
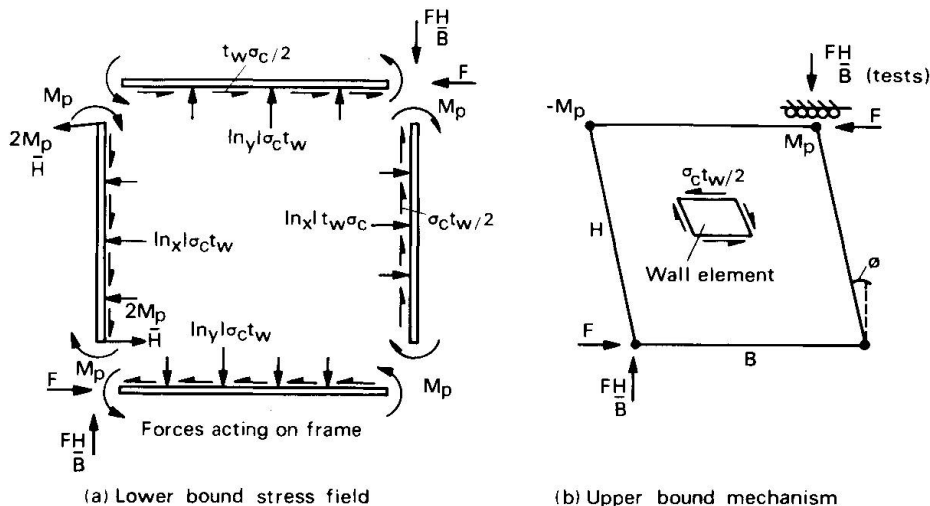


Fig 2 Yield criterion for orthogonally reinforced panel elements

The yield criterion assumed is due to Nielsen [4], shown in Fig 2, and outlined by Morley [5] and Marti [6]. It should be noticed that certain regions of the criterion introduce indeterminacy into the calculation of stress components corresponding to assumed strain rates via the flow rule. For upper bound solutions these components are usually accompanied by zero components of the strain-rate but for lower bound solutions, guided by the upper bound stress fields, this indeterminacy causes non-unique stress fields which satisfy equilibrium.

2.2 Composite shear mode S

Fig 3
Shear mode S



All modes will be examined with equal plastic moments in the beams and columns. The assumed mechanism (Fig 3b) has a dissipation of energy in the frame of $4M_p\phi$ provided that the joints are rigid. For small displacements a rectangular frame would not require any extension of the panel only pure shear. Reference to the yield criterion, Fig 2, shows that the stress point associated with a strain-rate $(0, 0, -\phi)$ is

$$\left(-(\frac{1}{2} + \alpha_x) \leq n_x \leq -(\frac{1}{2} - \alpha_x), -(\frac{1}{2} + \alpha_y) \leq n_y \leq -(\frac{1}{2} - \alpha_y); n_{xy} = \pm \frac{1}{2} \right)$$

The energy dissipated in the panel is thus $BH\phi t_w \sigma_c/2$ and the work equation leads to an upper bound collapse load of

$$F = 4M_p/H + \frac{1}{2}\sigma_c t_w B \quad (1)$$

The lower bound stress field is shown in Fig 3a where n_x and n_y are constrained to lie within the ranges

$$-(\frac{1}{2} + \alpha_x) \leq n_x \leq -(\frac{1}{2} - \alpha_x); -(\frac{1}{2} + \alpha_y) \leq n_y \leq -(\frac{1}{2} - \alpha_y)$$

By considering the equilibrium of the beams and columns it can be shown that

$$F = 4M_p/H + \frac{1}{2}\sigma_c t_w B \quad \text{ie equation (1)}$$

Thus equation (1) is an exact solution provided that M_p is not exceeded anywhere in any of the beams or columns. Consideration of the bending moment in the top beam shows that the minimum permissible plastic moment is reached when the shear force at the left hand end is zero, ie $2M_p/B - \frac{1}{2}|n_y|\sigma_c t_w B = 0$ $\quad (2)$

Introducing Wood's [3] definition of f and m ,

$$f = F/(4M_p/H + \frac{1}{2}\sigma_c t_w B); \quad M = 8M_p/\sigma_c t_w B^2$$

then $f = 1$ providing for the beam $m \geq 2|n_y|$

Similarly, examination of the column gives the condition as $m \geq 2|n_x|H^2/B^2$

Thus if either of these conditions are violated, negative hinges could appear in the beam and/or columns marking the termination of mode S . Hence it is the accompanying direct stresses which are responsible for the change from the pure shear mode.



2.3 Shear rotation mode SR

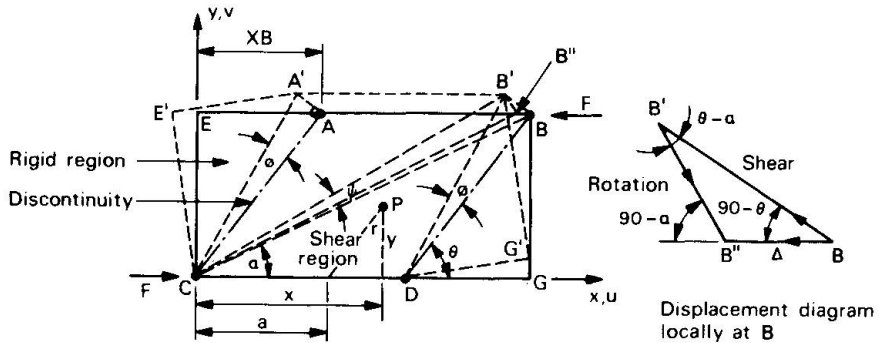


Fig 4 Mode SR upper bound

The negative moment hinge now appears at a point XB from the end E of the beam (Fig 4). The inclined discontinuities CA and DB separate the end rigid regions from the shearing region $ABCD$. Since CEA remains rigid it rotates to $CE'A'$ through an angle ϕ and the original rectangle is distorted to $CE'A'B'G'D$. However imposition of the boundary conditions requires a rigid body rotation of the whole panel through an angle ψ about C , so as to bring B' to B'' . As $\psi \ll \alpha$, $B'B''$ is virtually perpendicular to CB' , Fig 5, from which it can be shown that

$$\phi = \Delta \sin \theta \cos \alpha / (H \sin (\theta - \alpha)) \quad (3)$$

A further consequence of the discontinuities CA and DB is that there is expansion of the shear region in the y direction but none in the x direction.

From the displacement of a point P , Fig 4, the strain-rate in the shearing region can be deduced as

$$\epsilon_x = 0; \epsilon_y = \phi \cot \theta; \epsilon_{xy} = -\phi \quad (4)$$

Region D of the yield criterion, Fig 2, is able to support these strain-rate components and it can be shown that the stress point corresponding to (4) is given by

$$n_y = -(1 - 2a_y - \cos \theta)/2; n_{xy} = -(\sin \theta)/2$$

with n_x lying within the range

$$-(1 + 2a_x + \cos \theta)/2 \leq n_x \leq -(1 - 2a_x + \cos \theta)/2$$

Since the stresses and strain-rates are constant over an area $BH(1 - X)$ the dissipation of energy in the panel can be expressed as

$$D_w = \frac{1}{2} \sigma_c t_w \phi B H (1 - X) \left[\sin \theta - (1 - 2a_y - \cos \theta) \cot \theta \right] \quad (5)$$

Adding the frame dissipation, again $4M_p \phi$; equating to the external work $F\Delta$, and substituting for ϕ from (3), leads to

$$f = \left[B_m / H (1 - X) + \sqrt{1 + (BX/H)^2} - (1 - 2a_y) BX / H \right] / (1 + mB/H) \quad (6)$$

This equation is minimised numerically for X to obtain the best upper bound.

For the lower bound a stress point lying within region D of the yield criterion will be assumed. Such a point requires two parameters $n_x = -c_x$ and $n_y = -c_y$ since the shear component will be determined from the yield criterion's equations.

To ensure that the point remains within D , C_x and C_y must satisfy

$$C_y \leq (1 - \alpha_y) \text{ and } 1 - \alpha_x - \alpha_y \leq C_x + C_y \leq 1 + \alpha_x - \alpha_y \quad (7)$$

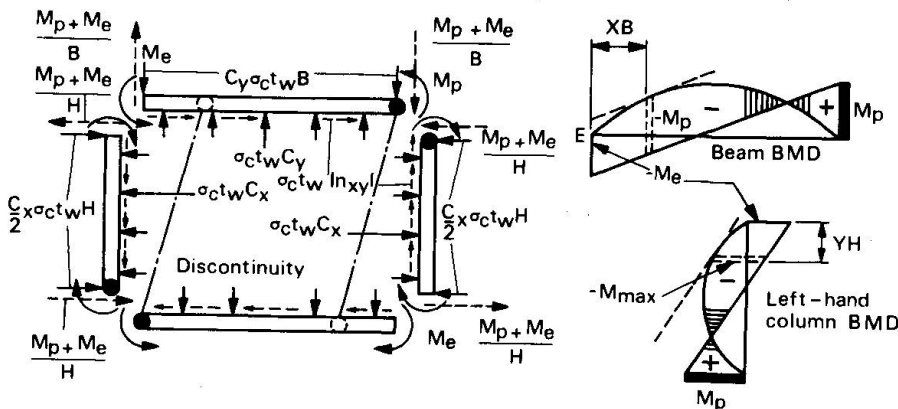


Fig 5 Mode SR lower bound

With this stress field the forces acting on the frame are as shown in Fig 5. Even though the discontinuity would permit a change in the stress component parallel to the discontinuity in the triangular regions, a continuous stress field is assumed throughout. A negative plastic moment is enforced in the beams at the ends of the discontinuities, resulting in the moment at the non-loaded beam-column junction no longer being plastic. For the solution, in addition to the three equilibrium conditions for each beam and column, there are two conditions relating to the position of the minimum moment in the beam. Firstly that this position has zero shear and secondly that this is a plastic moment. Solving these results in

$$X = 1 - \sqrt{m/2C_y} \quad (8)$$

$$M_e/M_p = 1 - 4C_y X^2/m \quad (9)$$

The columns must be checked to ensure that overstressing does not result and a section distance YH from the bottom of the right hand column is examined for minimum moment and zero shear. This results in

$$Y = \frac{1}{2} \left\{ 1 + (B^2/H^2) (C_y/C_x) (X^2 - m/2C_y) \right\} \quad (10)$$

$$M_{max}/M_p = 1 - 4C_x (1 - Y)^2 H^2 / m B^2 \quad (11)$$

Finally the expression for f is obtained as

$$f = 2 \left[C_y (1 - 2X) B/H + \sqrt{(1 - \alpha_y - C_y)(\alpha_y + C_y)} \right] / (1 + mB/H) \quad (12)$$

f is maximised numerically for trial C_x and C_y values within the range defined by equation (7) using the following strategy:

- (a) X must be in the range $0 \leq X \leq 1$.
- (b) M_e/M_p from (9) must be within the range -1 to $+1$.
- (c) If Y from (10) is positive then $|M_{max}/M_p| \leq 1$.
- (d) If Y is negative then the value returned for M_{max}/M_p is ignored.
- (e) If either M_e/M_p or M_{max}/M_p exceeds unity then a valid lower bound can still be obtained providing f is divided by the largest of these values.

From equations (10) and (11) C_x merely affects the degree and position of the

minimum moment in the columns. For a given C_y , any value of C_x is acceptable which satisfies (7) and conditions (c) and (d) above without generating (e) if possible. This is usually achieved by selecting the lower end value of the range.

Specimen results of the upper and lower bound solutions are shown in Table 1.

B/H	m	α_x	α_y	f_{LB}	f_{UB}
1	0.2	0.1	0.1	0.8333	0.9060
1	0.5	0.1	0.1	0.9766	0.9861
1	0.3	0.05	0.05	0.8763	0.9251
2	0.25	0.1	0.1	0.9210	0.9210
2	0.6	0.05	0.05	0.9867	0.9867

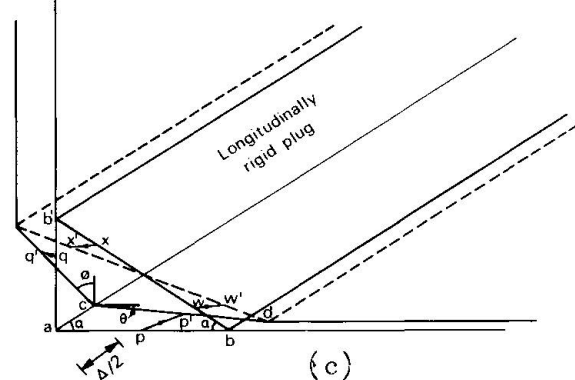
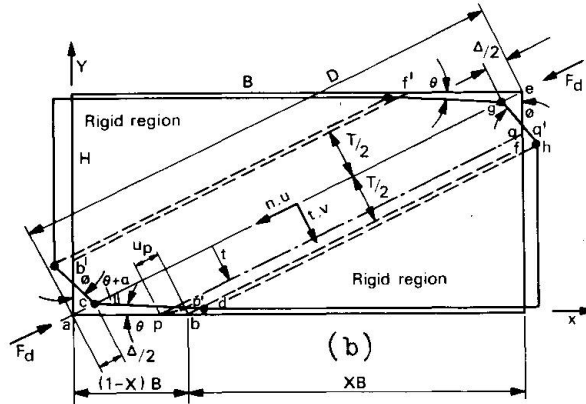
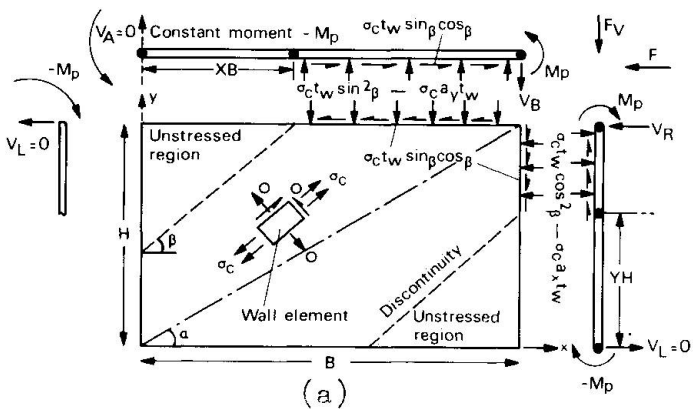
Table 1 Comparison of mode SR upper and lower bound solutions

2.4 Diagonal compression mode DC

The lower bound solution for this mode assumes that the distribution of load by the frame to the panel is such as to cause a diagonal band stressed to its maximum, leaving the remaining regions rigid and stress free. To allow for orthotropic reinforcement, a band orientated as shown in Fig 6a has been assumed allowing two parameters Y and X . However this solution, in general violates

Fig 6 Mode DC

- (a) Lower bound forces and moments $V_L = 0$
- (b) Upper bound mechanism
- (c) Enlarged corner detail for mechanism



global equilibrium requirements unless a band parallel to the panel diagonal is assumed resulting in a very restricted set of panel parameters for which the solution is valid. Thus a more general solution free from these restrictions, is required and is currently under investigation. Where the solution is valid X , Y and f are given by

$$X = 1 - \sqrt{m/2(\sin^2 \beta - \alpha_y)} \quad (13); \quad Y = 1 - \sqrt{mB^2/2H^2(\cos^2 \beta - \alpha_x)} \quad (14)$$

$$f = 2 \left[(1 - Y)(\cos^2 \beta - \alpha_x)H/B + (1 - X)\sin \beta \cos \beta \right] / (1 + mB/H) \quad (15)$$

Since the lower bound is restricted this is reflected in the upper bound mechanism, Figs 6b and 6c, which has a parallel diagonal band containing a

diagonally rigid region, so that crushing is confined to the triangular regions at opposite ends of this band. This rigid region is allowed to shear and expand transversely which is ensured by insisting that bb' and ff' , Fig 6c, rotate but remain parallel. Details of this mechanism can be found in Wood's paper [3] but modification is needed since the yield criterion requires the strain-rate components to be in the direction of the reinforcement bars and not parallel and perpendicular to the panel diagonal. Performing this transformation, and determining the corresponding stress points and resulting energy dissipation, in a similar manner to that for mode *SR*, results in

$$f = \left[1 + Bm/H(1 - X) - 2(1 - \alpha_x - \alpha_y)BX/H(1 + (B/H)^2) \right] / (1 + mB/H) \quad (16)$$

The minimum is found by differentiation and occurs when

$$X = 1 - \sqrt{m(1 + B^2/H^2)/2(1 - \alpha_x - \alpha_y)} \quad (17)$$

For solution purposes these equations are evaluated separately to ensure that X remains in the range $0 < X < 1$.

3. COMPARISON OF THE UPPER AND LOWER BOUND SOLUTIONS

Plotted curves of the various solutions proved to be overlapping and confusing, as indicated by the lower bound solutions for square panels having isotropic reinforcement, Fig 7. The trend of solutions has thus been indicated by tabulating the best solutions for $\alpha_x = 0.1$, $\alpha_y = 0.1$, with a code to indicate which mode applies, Table 2. Unlike the unreinforced case, there are no analytical expressions valid throughout the range of m , nor are there any analytically exact solutions. For non-square panels mode *SR* solutions are numerically exact to ten decimal places, providing that the lower bound has not been modified due to column overstress. For square panels with isotropic reinforcement, mode *SR* lower bound is numerically equal to mode *DC* upper bound until, again, column overstress causes a rapid fall off in the *SR* lower bound, Fig 7, which is then superseded by the mode *DC* lower bound. This result is due to the symmetry of this case since a plastic hinge would be expected to form in the column also; a fact confirmed by noting that the best lower bound for *SR* occurs when the column overstress factor is unity.

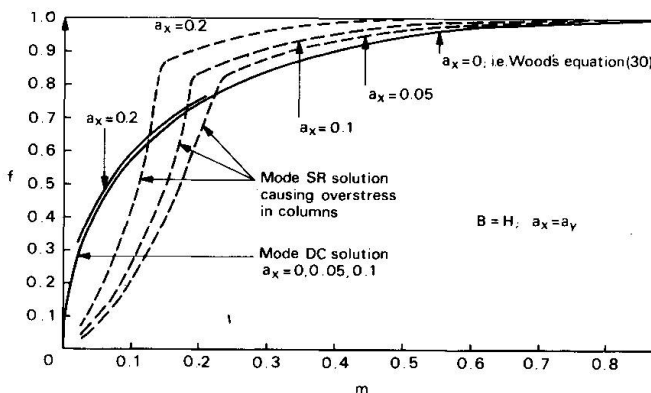


Fig 7 Lower bound solutions for square panels with isotropic reinforcement

m	Best lower bound for f		Best upper bound for f	
	$B/H = 1$	$B/H = 2$	$B/H = 1$	$B/H = 2$
0.8	1.0 <i>S</i>	1.0 <i>S</i>	1.0 <i>S</i>	1.0 <i>S</i>
0.6	0.9910 <i>SR</i>	0.9944 <i>SR</i>	0.9910 <i>DC</i>	0.9944 <i>SR</i>
0.4	0.9510 <i>SR</i>	0.9693 <i>SR</i>	0.9510 <i>DC</i>	0.9693 <i>SR</i>
0.25	0.8755 <i>SR</i>	0.9210 <i>SR</i>	0.8755 <i>DC</i>	0.9210 <i>SR</i>
0.2	0.8333 <i>SR</i>	0.8938 <i>SR</i>	0.8333 <i>DC</i>	0.8938 <i>SR</i>
0.15	0.6778 <i>DC</i>	0.8566 <i>SR</i>	0.7764 <i>DC</i>	0.8574 <i>SR</i>
0.1	0.5785 <i>DC</i>	0.7940 <i>SR</i>	0.6961 <i>DC</i>	0.8069 <i>SR</i>
0.05	0.4286 <i>DC</i>	0.3684 <i>SR</i>	0.5714 <i>DC</i>	0.7331 <i>SR</i>

Table 2 Example of the best upper and lower bound solutions

For rectangular panels and for square panels with orthotropic reinforcement, the general solution is hampered by the restrictions placed on the validity of the mode *DC* lower bound, but even where this solution is valid, eg Fig 7, there is a considerable jump between the solutions for modes *DC* and *SR*, suggesting that



there are better solutions for panels having small m values. For square panels with orthotropic reinforcement, the trend from the number of cases evaluated to date is that as well as both SR solutions being unequal, the equality between SR lower bound and DC upper bound has disappeared.

4. CONCLUSION

An introduction of plasticity analysis to reinforced concrete panels in frames has been achieved by assuming that the modes observed for unreinforced panels are applicable. For single panels having equally strong beams and columns analytically exact solutions for the pure shear mode S have been obtained for all panels; numerically exact solutions for the shear-rotation mode SR have been obtained for rectangular panels and for square panels having isotropic reinforcement, and a very restrictive set of conditions has been determined for which the diagonal compression mode DC is valid. This latter point suggests that either there are better solutions for this mode or that a more suitable mode exists.

5. NOTATION

A_x, A_y area of reinforcement in the co-ordinate directions per unit width of panel.

σ_y magnitude of the yield stress of the reinforcement bars.

N_x, N_y, N_{xy} membrane forces per unit width of panel element.

$$n_x = \frac{N_x}{\sigma_c t_w} \quad n_y = \frac{N_y}{\sigma_c t_w} \quad n_{xy} = \frac{N_{xy}}{\sigma_c t_w} \quad a_x = \frac{A_x \sigma_y}{\sigma_c t_w} \quad a_y = \frac{A_y \sigma_y}{\sigma_c t_w}$$

6. ACKNOWLEDGEMENT

This paper is published by permission of the Director of the Building Research Establishment and forms part of the current research programme. The author is indebted to Dr R H Wood, formerly of the Building Research Establishment, for his invaluable help during this work.

7. REFERENCES

- 1 WOOD, R H. The stability of tall buildings. *Proc Instn Civ Engrs*, 11, Sept, (1958), 69-102
- 2 MAINSTONE, R J and WEEKS, G A. The influence of a bounding frame on the racking stiffnesses and strengths of brick walls. *Proc 2nd Int Brick Masonry Conf*, (1970), 165-171
- 3 WOOD, R H. Plasticity composite action and collapse design of unreinforced shear wall panels in frames. *Proc Instn Civ Engrs*, Part 2, 65, June, (1978), 381-411
- 4 NIELSEN, M P. On the strength of reinforced concrete discs. *Acta Polytech Scand.*, Series 70, Bulletin 2, (Copenhagen), (1971)
- 5 MORLEY, C T. Yield criteria for elements of reinforced concrete slabs. *Plasticity in Reinforced Concrete, Introductory Report*, IABSE Colloquium, Zurich, (1979), 35-47
- 6 MARTI, P. Plastic analysis of reinforced concrete shear walls. *Plasticity in Reinforced Concrete, Introductory Report*, IABSE Colloquium, Zurich, (1979), 51-69